

Three Polymorphs of 2-Amino-5-nitropyrimidine: Experimental Structures and Theoretical Predictions

Christer B. Aakeröy,* Mark Nieuwenhuyzen,† and Sarah L. Price‡

Contribution from the Department of Chemistry, Kansas State University, Manhattan, Kansas, 66506, School of Chemistry, David Keir Building, The Queen's University of Belfast, Belfast, BT9 5AG, Northern Ireland, and Centre for Theoretical and Computational Chemistry, University College London, 20 Gordon Street, London WC1H 0AJ, U.K.

Received April 3, 1998

Abstract: Three previously unknown crystal structures (polymorphs) of 2-amino-5-nitropyrimidine (**I–III**), as determined by single-crystal X-ray diffraction, are reported. Crystal packing, hydrogen-bond patterns, and intermolecular forces have been examined in detail, and theoretical studies were performed on **I–III** to estimate their lattice energies and to determine the role of changes in molecular conformation upon the resulting crystal structure. Each structure is characterized by an extensive network of hydrogen bonds (including C–H···N and C–H···O interactions) and short interlayer distances. This structural system has shown up limitations of several assumptions that are generally made in current methods of predicting crystal structures and polymorphism, but within these limitations, the applied scheme has been successful.

Introduction

One of the most challenging aspects of crystal engineering¹ arises from the fact that many compounds are polymorphic.² To predict packing motifs and crystal structures of unknown compounds, we are not only required to rationalize the structural effects of a range of intermolecular forces, but we also need to account for the possible appearance of alternative packing patterns in compounds of interest.

Although there is much debate about whether polymorphism is pervasive or not, there is no doubt that, from a materials perspective, the structural composition and homogeneity of a crystalline sample is of equal importance to its chemical purity. Polymorphism³ introduces “impurities” into a crystalline material that are impossible to detect with solution-based analytical methods, and this can lead to disturbing scenarios where new structural phases can be incorporated into commercial products and formulations at an advanced stage of processing, long after the chemical composition has been established beyond doubt. The presence of such “structural impurities” can be very detrimental to the physical properties and performance of many speciality chemicals. Although polymorphism has been studied most extensively in the pharmaceutical industry (a large proportion of drug substances have been shown to be polymorphic⁴), structural homogeneity may also have decisive effects on production, performance, and long-term stability of an enormous variety of solids, viz., colorants and pigments,

agrochemicals, explosives, propellants, and nonlinear optical materials. Consequently, recent years have witnessed many efforts aimed at explaining and predicting the existence of polymorphic structures,^{5–7} and improvements in computational techniques have led to the developments of programs which aim to predict the crystal structures, and thus possible polymorphism, of organic compounds.^{8,9} Despite some success, the field is still in its infancy and more experimental data and theoretical studies are required.

Polymorphic systems provide unique opportunities to study competition between intermolecular forces and correlations between changes in molecular structure and crystal packing, but it is rare to have full crystal structure determinations of three polymorphs, performed at the same time. Indeed Gavezzotti and Filippini¹⁰ only found 16 examples of molecules with three or more polymorphs in the Cambridge Structural Database.¹¹ Thus, the series of structures presented herein allows (i) an assessment of how intramolecular flexibility and conformational demands affect the structure and packing of polymorphs and (ii) an examination of the strength, energetics, and structural influence of intermolecular interactions upon the resulting structure.

(5) Gallagher, H. G.; Roberts, K. J.; Sherwood, J. N.; Smith, L. A. *J. Mater. Chem.* **1997**, *7*, 229. Davey, R. J.; Blagden, N.; Potts, G. D.; Docherty, R. *J. Am. Chem. Soc.* **1997**, *119*, 1767.

(6) Price, S. L.; Wibley, K. S. *J. Phys. Chem. A* **1997**, *101*, 2198.

(7) Gavezzotti, A. *Acc. Chem. Res.* **1994**, *27*, 309.

(8) Karfunkel, H. R.; Gdanitz, R. *J. Comput. Chem.* **1992**, *13*, 1171. Gavezzotti, A. *J. Am. Chem. Soc.* **1991**, *113*, 4622. Hofmann, D. W. M.; Lengauer, T. *Acta Crystallogr., Sect. A* **1997**, *53*, 225. Van Eijck, B. P.; Mooij, W. T. M.; Kroon, J. *Acta Crystallogr., Sect. B* **1995**, *51*, 99. Chaka, A. M.; Zaniewski, R.; Youngs, W.; Tessier, C.; Klopman, G. *Acta Crystallogr., Sect. B* **1996**, *52*, 165. Tajima, N.; Takayuki, T.; Arikawa, T.; Sakurai, T.; Teramae, S.; Hirano, T. *Bull. Chem. Soc. Jpn.* **1995**, *68*, 519. Gdanitz, R. *J. Chem. Phys. Lett.* **1992**, *190*, 391. Williams, D. E. *Acta Crystallogr., Sect. A* **1996**, *52*, 326.

(9) Holden, J. R.; Du, Z.; Ammon, H. L. *J. Comput. Chem.* **1993**, *14*, 422.

(10) Gavezzotti, A.; Filippini, G. *J. Am. Chem. Soc.* **1995**, *117*, 12299.

(11) Allen, F. H.; Kennard O. *Chem. Des. Automation News* **1993**, *8*, 3137.

* Kansas State University. E-mail: aakeroy@ksu.edu.

† The Queen's University of Belfast.

‡ University College London. E-mail: s.l.price@ucl.ac.uk.

(1) Desiraju, G. *Crystal Engineering: The Design of Organic Solids*; Elsevier: New York, 1989. Desiraju, G. R. *Angew. Chem., Int. Ed. Engl.* **1995**, *34*, 2311. Aakeröy, C. B. *Acta Crystallogr., Sect. B* **1997**, *53*, 569.

(2) Deffet, L. *Repertoire de Composés Organiques Polymorphes*, Liege, 1942. Pfeiffer, P. *Organische Molekülverbindungen*, 2nd ed.; Verlag von Ferdinand Enke: Stuttgart, 1927. Groth, P. *Chemische Kristallographie*; Verlag von Wilhelm Engelmann: Leipzig, 1910; Vol. III–V.

(3) Halebian, J.; McCrone, W. J. *Pharm. Sci.* **1969**, *58*, 911.

(4) Grunenberg, A. *Regelweiterbildungssseminar Pharmazeutische Analytik*; Bonn, 1992; pp 1–8.

Model System and Objectives. The increasing interest in molecular recognition and crystal engineering has brought considerable attention to substituted pyrimidines in view of their ability to engage in robust hydrogen-bond interactions. Notably, Etter et al.¹² have described how 2-aminopyrimidine can be used to probe the hydrogen-bond preferences of carboxylic acids, and this work has led to several design strategies of low-dimensional assemblies in the organic solid state.¹³ Suitably substituted heterocyclic molecules can also have large molecular nonlinear polarizabilities which may render them useful for new nonlinear optical (NLO) materials. However, this requires a favorable orientation of molecules in a crystal lattice which again emphasizes the importance of structure and intermolecular forces. Although 2-amino-5-nitropyrimidine has been structurally characterized and the corresponding cation has been used extensively in NLO materials,¹⁴ no crystallographic data for the analogous pyrimidine have been reported. Our investigation of 2-amino-5-nitropyrimidine found three polymorphic forms, enabling us to present a structural and theoretical study which provides further insight into the phenomenon of polymorphism and illustrates the strengths and weaknesses of current computational methods of predicting the crystal structures of organic molecular solids.⁷⁻⁹

2-Amino-5-nitropyrimidine is an attractive molecule both from a materials/crystal engineering and from a structural/theoretical perspective: (i) it has a large molecular dipole moment and may be incorporated in new NLO-materials, (ii) it contains several potential donors and acceptors for both weak, C-H...X, and strong, N-H...X, (X = O or N) hydrogen-bond interactions; (iii) it is small enough to make it accessible to ab initio methodologies; (iv) reliable potentials for calculations of lattice energies of such compounds are available; and (v) the molecule has relatively limited conformational flexibility. Previous computational studies include ab initio SCF calculations of the molecular electrostatic potentials around 2-aminopyrimidine and 2-aminopyrimidine,¹⁵ and a study of intermolecular interactions in 2-amino-5-nitropyrimidine (form I) and 2-amino-5-nitropyrimidine.¹⁶ Our structure determinations of three polymorphs of 2-amino-5-nitropyrimidine were accompanied by ab initio and lattice energy calculations to determine the role of the changes in molecular conformation on the crystal structure.

The crystal structure modeling was performed using a novel intermolecular potential scheme which has been used successfully for several polar C/H/N/O organic molecules,^{17,18} including molecules based on aromatic rings with both amine and nitro substituents which are closely related to 2-amino-5-nitropyrimidine. Over 40 crystal structures have been satisfactorily reproduced within the limitations of a static lattice energy minimization model.¹⁷ The model intermolecular potentials use a distributed multipole model, allowing the electrostatic energy to be calculated from sets of atomic charges, dipoles, quadru-

poles, etc., which represent the ab initio charge density of the molecule. Thus the electrostatic forces, which dominate the orientation dependence of the potential, are modeled particularly realistically, and include the electrostatic effects of features such as lone pair and π -electron density on hydrogen bonding, and π - π stacking interactions. The theoretical basis of the electrostatic model ensures that it is equally reliable at all orientations sampled in both experimental and hypothetical crystal structures.

The effect of the slight conformational variations between the polymorphs was studied by modeling the crystal structures with both the experimental and an idealized molecular structure, obtained by ab initio optimization. Such an assumed molecular structure would have to be used in any study seeking to predict the polymorphs of a molecule prior to synthesis, and provides a molecular structure which is unbiased by the effects of crystal packing in any particular polymorph. A limited attempt to predict polymorphism of 2-amino-5-nitropyrimidine was also made, through a combination of the usual assumption that the observed structures correspond to low-lying minima in the static lattice energy and a recently proposed method for searching the multidimensional space of possible crystal structures.⁹

Experimental Section

Sample Preparation. Form I. 2-Amino-5-nitropyrimidine was sublimed at ambient pressure to yield small, near-colorless, diamond-shaped crystals.

Form II. 2-Amino-5-nitropyrimidine was recrystallized at ambient temperature from ethanol. Slow evaporation of the solvent resulted in the precipitation of colorless needlelike crystals. The same polymorphic form is also obtained by recrystallization from a hot aqueous solution; upon cooling at ambient temperature, very long needlelike crystals are formed.

Form III. 2-Amino-5-nitropyrimidine was recrystallized at ambient temperature from acetone. Slow evaporation of the solvent resulted in the precipitation of colorless blocklike crystals.

Several other solvents were also tried for recrystallization, in addition to a variety of vapor diffusion and liquid diffusion experiments. We were unable to identify any other polymorphs than those described above, I-III.¹⁹

X-ray Crystallography. Crystal data were collected using a Siemens P4 four-circle diffractometer with graphite monochromated Mo K α radiation, Table 1. Crystal stability was monitored by measuring standard reflections every 100 reflections, and there were no significant variations (<±1%). Cell parameters were obtained from 35 accurately centered reflections in the 2θ range 10–25°. ω scans were employed for data collection and Lorentz and polarization corrections were applied. The structures were solved by direct methods and the nonhydrogen atoms were refined with anisotropic thermal parameters. Hydrogen-atom positions were located experimentally from difference Fourier maps, and their thermal parameters were subsequently obtained using a riding model with fixed thermal parameters ($U_{ij} = 1.2U_{eq}$ for the atom to which they are bonded). The function minimized was $\sum [\omega(|F_o|^2 - |F_c|^2)]$ with reflection weights $\omega^{-1} = [\sigma^2|F_o|^2 + (g_1P)^2 + (g_2P)]$, where $P = [\max |F_o|^2 + 2|F_c|^2]/3$. The SHELXTL PC and SHELXL-93 packages were used for data reduction and structure solution and refinement.²⁰

(19) We did observe forms I-III of 2-amino-5-nitropyrimidine during an attempt to make cocrystals with 2-aminopyrimidine (two forms based upon the latter compound were also identified). The starting materials were dissolved in a 1:1 ratio in butanol. Upon evaporation through slow evaporation, five distinctive crystalline materials were obtained: (i) 2-amino-5-nitropyrimidine (yellow plates); (ii) 2-amino-5-nitropyrimidine hydrate (yellow/colorless dichroic blocks); (iii) 2-amino-5-nitropyrimidine I (thick diamond shaped plates); (iv) 2-amino-5-nitropyrimidine II (white needles); and (v) 2-amino-5-nitropyrimidine III (colorless blocks).

(20) Sheldrick, G. M. SHELXL-93; University of Göttingen: Göttingen, Germany.

(12) Etter, M. C.; Adson, D. A. *J. Chem. Soc., Chem. Commun.* **1990**, 589.

(13) Smith, G.; Gentner, J. M.; Lynch, D. E.; Byriel, K. A.; Kennard, C. H. L. *Aust. J. Chem.* **1995**, *48*, 1151.

(14) Nicoud, J.-F.; Masse, R.; Bourgoigne, C.; Evans, C. *J. Mater. Chem.* **1997**, *7*, 35. Pecaut, J.; Le Fur, Y.; Masse, R. *Acta Crystallogr., Sect. B* **1993**, *49*, 535. Le Fur, Y.; Bagieu-Beucher, M.; Masse, R.; Nicoud, J.-F.; Levy, J.-P. *Chem. Mater.* **1996**, *8*, 68. Bagieu-Beucher, M.; Masse, R.; Tran Qui, D. *Z. Anorg. Allg. Chem.* **1991**, *606*, 59.

(15) Politzer, P.; Kirschenheuter, G. P.; Miller, R. S. *J. Phys. Chem.* **1988**, *92*, 1436.

(16) Stone, A. J.; Tsuzuki, S. *J. Phys. Chem. B* **1997**, *101*, 10178.

(17) Coombes, D. S.; Price, S. L.; Willock, D. J.; Leslie, M. *J. Phys. Chem.* **1996**, *100*, 7352.

(18) Coombes, D. S.; Nagi, G. K.; Price, S. L. *Chem. Phys. Lett.* **1997**, *265*, 532.

Table 1. Data Collection and Refinement for Forms I–III of 2-Amino-5-nitropyrimidine

crystal data	I	II	III
empirical formula	C ₄ H ₄ N ₄ O ₂	C ₄ H ₄ N ₄ O ₂	C ₄ H ₄ N ₄ O ₂
MW	140.11	140.11	140.11
crystal size (mm)	0.74 × 0.33 × 0.09	0.69 × 0.34 × 0.23	0.81 × 0.32 × 0.21
crystal system	monoclinic	monoclinic	orthorhombic
space group	<i>P</i> 2 ₁ / <i>c</i>	<i>P</i> 2 ₁ / <i>n</i>	<i>P</i> ccn
<i>a</i> (Å)	5.128(1)	3.554(1)	4.165(1)
<i>b</i> (Å)	17.500(2)	16.524(6)	6.654(1)
<i>c</i> (Å)	6.872(1)	9.465(4)	21.293(4)
β	104.37(1)	99.00(2)	
volume (Å ³)	597.4(1)	549.0(3)	590.1(2)
<i>Z</i>	4	4	4
<i>D</i> _{calc} (g cm ⁻³)	1.558	1.695	1.577
<i>F</i> (000)	288	288	288
μ (Mo K α (mm ⁻¹))	0.130	0.140	0.130
temp (K)	120	123	123
ω scans; θ range/ $^\circ$	2.33–25.0	2.47–25.0	3.61–24.97
range <i>h</i>	–1 to 6	–4 to 2	–1 to 4
range <i>k</i>	–1 to 20	–1 to 19	–1 to 7
range <i>l</i>	–8 to 8	–11 to 11	–1 to 25
reflns collected	1518	1802	821
unique reflns	1048	968	518
data:parameter ratio	11.51	10.63	10.79
<i>R</i> / <i>R</i> _w (obs data)	0.0515/0.0926	0.0322/0.0836	0.0331/0.0868
<i>R</i> / <i>R</i> _w (all data)	0.1220/0.1212	0.0384/0.0882	0.0387/0.0917
$\Delta\rho_{\text{max/min}}$ (e Å ⁻³)	0.139/–0.162	0.149/–0.246	0.147/–0.222
<i>S</i>	1.004	1.119	1.097

Computational Methods. Two types of crystal model were constructed for each polymorph of 2-amino-5-nitropyrimidine, using different molecular structures. The EXPTL crystal model used the experimental structure of the molecule in each polymorph, corrected for the inadequacies of X-ray determination by positioning the hydrogen atoms at a standard bond length of 1.08 Å for C–H and 1.01 Å for N–H along the experimental bond direction.²¹ Second, the IDEAL crystal model used the ab initio optimized molecular structure positioned in each experimental lattice to match the positions of origin and the orientation of the local axes system of each molecule in the unit cell. The right-handed orthogonal local axis system for each molecule has the origin at the center of mass, the *x*-axis parallel to the C(5)⋯C(2) vector and the *y*-axis in the plane containing C(5), C(2), and C(4). The differences in the molecular structures not only change the positions of the interaction sites, but the electrostatic model also reflects the changes in the charge distribution with structure, as the electrostatic model was obtained from the wave function of each molecular structure. However, as noted in the discussions below, the variations observed in the molecular structures in the three polymorphs were small.

The gas-phase IDEAL structure of the molecule was found by optimizing the energy of a SCF 6-31G** wave function, assuming *C*_{2v} symmetry, within the program CADPAC.²² An MP2 6-31G** wave function for each of the molecular structures was subject to a distributed multipole analysis (DMA),²³ to provide a set of multipoles up to hexadecapole on each nuclear site to represent the charge density.

The intermolecular potential used in the crystal modeling comprised an empirical 6-exp repulsion-dispersion model, plus the electrostatic energy calculated from the DMA of the relevant molecular structure, using all terms in the atom–atom multipole expansion up to *R*⁻⁵ (thus including the quadrupole–quadrupole interaction from the π electrons). The intermolecular potential between every pair of molecules in the crystal had the form:

(21) Allen, F. H.; Kennard, O.; Watson, D.G.; Brammer, L.; Orpen, A. G.; Taylor, R. *J. Chem. Soc., Perkin Trans. 2* **1987**, S1–S19.

(22) Amos, R. D., with contributions from Alberts, J. A.; Colwell, S. M.; Handy, N. C.; Jayatilaka, D.; Knowles, P. J.; Kobayashi, R.; Koga, N.; Laidig, K. E.; Maslen, P. E.; Murray, C. W.; Rice, J. E.; Sanz, J.; Simandiras, E. D.; Stone, A. J.; Su, M. D. *CADPAC5: The Cambridge Analytical Derivatives Package*, 1992, Cambridge.

(23) Stone, A. J.; Alderton, M. *Mol. Phys.* **1985**, *56*, 1047.

$$U_{AB} = \sum_{i \in A, j \in B} A_{ik} \exp(-B_{ik} R_{ik}) - C_{ik}/R_{ik}^6 + U_{\text{electrostatic}}(\text{DMA}, R^{-n}_{ik}, n = 1, 5)$$

where atoms *i* and *k* on molecules *A* and *B*, respectively, are of atomic types ι and κ . The repulsion-dispersion parameters for C, H, N, and O (see Supporting Information) were derived by Williams and co-workers by fitting to crystal data for azabenzene²⁴ and oxo hydrocarbons.²⁵ Parameters for the polar hydrogen atoms H_p were derived by fitting, within this potential scheme, to a range of polar N–H⋯O/N hydrogen bonded crystals and their enthalpies of sublimation, and the total model potential scheme validated for a wide range of crystal structures of related molecules.¹⁷ The program DMAREL²⁶ was used to minimize the lattice energy calculated from this model potential, by optimizing the cell constants and the translation and rotation of each rigid molecule in the unit cell to remove the cell strains, forces, and torques by a pseudo-Newton-Raphson technique. The charge-charge, charge-dipole, and dipole-dipole contributions to the electrostatic lattice energy were evaluated by an Ewald summation, with all other terms evaluated by direct summation with a cutoff of 20 Å.

An attempt was made to predict the low-energy crystal structures of 2-amino-5-nitropyrimidine, using the IDEAL molecular geometry. The program MOLPAK⁹ was used to generate starting points for lattice energy minimization with the above potential, by searching for close-packed crystal structures using a simple repulsive potential, in the most common coordination geometries found in organic crystals. The initial MOLPAK search considered structures with one entire molecule in the asymmetric unit within space groups *P* $\bar{1}$, *P*2₁, *P*2₁/*c*, *P*2₁2₁2₁, *P*1, *C*2/*c*, *P*na2₁, and *P*bca, generating approximately 20 × 25 = 500 hypothetical dense crystal structures. Over 300 of these initial structures were energy minimized using DMAREL with the model potential, concentrating on the most common space groups (*P* $\bar{1}$, *P*2₁, *P*2₁/*c*, *P*2₁2₁2₁) and those with *P*2₁/*c* as a subgroup, but also including all of MOLPAK generated geometries with an initial lattice energy below –50 kJ mol⁻¹. It is important to note that the nearest such a method can come to any experimental structure is to locate the same minimum in the lattice energy as found starting from the experimental structure, using the IDEAL molecular structure.

Results

Experimental Crystal Structures. The relevant X-ray crystallographic information is presented in Table 1. Numbering schemes, molecular geometries, and thermal ellipsoids of I–III are presented in Figure 1.

Form I crystallizes in the monoclinic centrosymmetric space group *P*2₁/*c* with no unexpected intramolecular bond distances. The nitro group is coplanar with the aromatic ring, whereas the amino group is slightly twisted out of the plane due to a small degree of pyramidalization of the amino group. The two exocyclic C–N bond distances are unexceptional and fall within the range of typical C–N(amino) and C–N(nitro) distances observed for other aromatic nitroamino compounds.¹¹

The structure displays extensive hydrogen bonding, Table 2, and every possible atom of the molecule participates as either a hydrogen-bond donor or acceptor, Figure 2a. There are four unique hydrogen bonds in this structure which generate infinite 2-D layers approximately parallel with the (–102) plane, Figure 2b. Two notable “dimeric” interactions exist within each layer generated by pairs of symmetry related N(2)–H(21)⋯N(1) and C(4)–H(4)⋯N(3) hydrogen bonds. The former interaction generates a R₂² (8) motif²⁷ which is commonly observed with 2-amino pyridine moieties, and the latter R₂² (6) motif has been

(24) Williams, D. E.; Cox, S. R. *Acta Crystallogr., Sect. B* **1984**, *40*, 404.

(25) Cox, S. R.; Hsu, L. Y.; Williams, D. E. *Acta Crystallogr., Sect. A* **1981**, *37*, 293.

(26) Willock, D. J.; Price, S. L.; Leslie, M.; Catlow C. R. A. *J. Comput. Chem.* **1995**, *16*, 628.

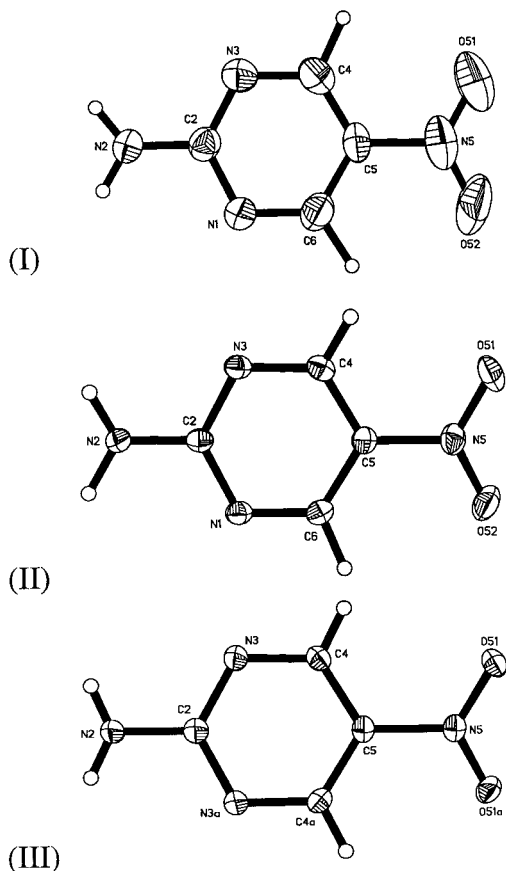


Figure 1. Geometries, thermal ellipsoids (50%), and atom numbering schemes of 2-amino-5-nitropyrimidine for forms I–III.

Table 2. Geometry of the Hydrogen Bonds for Forms I–III of 2-Amino-5-nitropyrimidine^a

D–H···A	$r(\text{H}\cdots\text{A})/\text{\AA}$	$r(\text{D}\cdots\text{A})/\text{\AA}$	$\angle(\text{D}–\text{H}\cdots\text{A})/\text{deg}$
Form I			
N2–H21···N1 ⁱ	2.115(4)	3.003(4)	171.78(10)
N2–H22···O52 ⁱⁱ	2.154(4)	2.981(4)	157.40(12)
C4–H4···N3 ⁱⁱⁱ	2.496(4)	3.452(4)	144.72(11)
C6–H6···O51 ^{iv}	2.278(5)	3.364(5)	163.67(13)
Form II			
N2–H21···N1 ⁱ	1.959(2)	2.977(2)	173.98(5)
N2–H22···O52 ⁱⁱ	2.287(2)	3.043(2)	140.23(5)
C4–H4···N3 ⁱⁱⁱ	2.595(2)	3.355(2)	139.33(4)
C6–H6···O51 ^{iv}	2.306(2)	3.291(2)	167.03(5)
Form III			
N2–H22···N3 ⁱ	2.208(1)	3.046(1)	173.64(5)
C4–H4···O51 ⁱⁱ	2.505(2)	3.376(2)	155.37(4)

^a Symmetry codes: **Form I:** (i) $-x, -y, -z$; (ii) $-1-x, -1/2+y, -1/2-z$; (iii) $-2-x, -y, -1-z$; (iv) $1+x, 1/2-y, 1/2+z$. **Form II:** (i) $-x, 1-y, -z$; (ii) $1/2-x, -1/2+y, 1/2-z$; (iii) $-1-x, 1-y, 1-z$; (iv) $1/2+x, 1/2-y, -1/2+z$. **Form III:** (i) $-x, 1-y, -z$; (ii) $-1/2+x, 1-y, 1/2-z$.

observed in polymorphs of pyrazine carboxamide.²⁸ The interplanar separation is unusually small, with the shortest interplanar contact of approximately 3.26 Å for C2···C2' ($\ell = -1-x, -y, -z$), Figure 2b (the interplanar separation is 3.35 Å in graphite). Neighboring layers are organized such that the amino group in one layer is positioned over the center of an aromatic ring in the adjacent layer.

(27) For information about graph-set notation, see: Bernstein, J.; Davis, R. E.; Shimoni, L.; Chang, N.-L. *Angew. Chem., Int. Ed. Engl.* **1995**, *34*, 1555. Etter, M. C.; MacDonald, J. C.; Bernstein, J. *Acta Crystallogr., Sect. B* **1990**, *B46*, 256.

(28) Leiserowitz, L. *Acta Crystallogr., Sect. B* **1976**, *32*, 775.

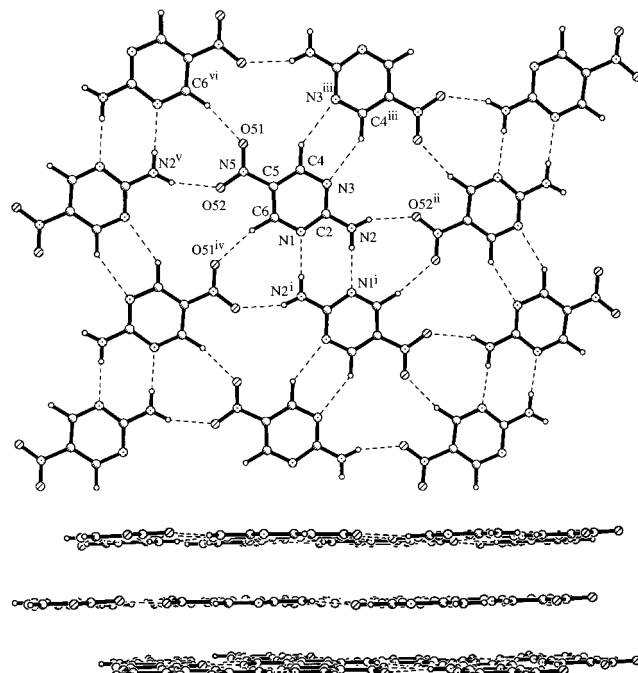


Figure 2. (a, top) Schematic view of the infinite 2-D hydrogen bonded layer for form I. Symmetry codes for nearest neighbors are (i) $-x, -y, -z$; (ii) $-1-x, -1/2+y, -1/2-z$; (iii) $-2-x, -y, -1-z$; (iv) $1+x, 1/2-y, 1/2+z$; (v) $-1+x, 1/2+y, -1/2-z$; (vi) $-1+x, 1/2-y, -1/2+z$. (b, bottom) Edge-on view showing the planar nature of the individual layers; dotted lines indicate hydrogen bonds.

Form II crystallizes in the monoclinic centrosymmetric space group $P2_1/n$ with no unexpected intramolecular bond distances.²⁹ The molecular structure of 2-amino-5-nitropyrimidine in **II** is very similar to that displayed in **I**, with the nitro group coplanar with the ring and a small degree of pyramidalization of the amino moiety. The hydrogen-bond pattern displayed in **II** is identical with that observed for form **I**, Table 2, and every potential hydrogen bond donor/acceptor atom participates in the formation of an infinite 2-D sheet, Figure 3a. The same hydrogen-bonded “dimeric” $R_2^2(8)$ and $R_2^2(6)$ motifs are present in both **I** and **II**. Contrary to **I**, however, the topology of the sheet in **II** is buckled (with a tilt of approximately 33°), which yields a more densely packed structure ($D_c = 1.695 \text{ g cm}^{-3}$ for **II** and $D_c = 1.558 \text{ g cm}^{-3}$ for **I**), Figure 3b. The perpendicular intermolecular plane separation is very small because of the offset between adjacent layers, with the shortest interplanar contacts, N(3)···C(4)' and N(3)···H(4)' of 3.09 and 2.82 Å respectively ($\ell = -x, 1-y, 1-z$).

Form III crystallizes in the orthorhombic centrosymmetric space group $Pccn$ with unremarkable intramolecular bond lengths and bond angles. The amino group is coplanar with the ring whereas the nitro group is twisted by 16° with respect to the aromatic ring. **Form III** displays a very different packing arrangement compared to **I** and **II**, and instead of a layered network, infinite hydrogen-bonded ribbons (twisted by ca. 68° with respect to each other) are running through the structure, Figure 4a. These ribbons are generated by pairs of symmetry related N–H···N hydrogen bonds, Table 2; this particular $R_2^2(8)$ “dimeric” interaction is present in all three polymorphs of 2-amino-5-nitropyrimidine, whereas the dimeric C(4)–H(4)···N(3) motif is only present in **I** and **II**. Neighboring ribbons

(29) It should be noted that although forms **I** and **II** have different unit cells, the symmetry relating molecules to one another is the same for both, as the space groups $P2_1/n$ and $P2_1/c$ have the same symmetry with different cell settings.

Table 3. Lattice Energy Minimizations Starting from Experimental Crystal Structures^a

crystal structure	I			II			III			
	molecular structure	X-ray	EXPTL	IDEAL	X-ray	EXPTL	IDEAL	X-ray	EXPTL	IDEAL
space group	<i>P2₁/c</i>				<i>P2₁/n</i>			<i>Pccn</i>		
<i>a</i> (Å)	5.128	4.968	4.999	3.554	3.874	4.999	4.165	4.163	5.331	
<i>b</i> (Å)	17.500	17.632	17.569	16.524	17.394	17.569	6.654	6.470	5.331	
<i>c</i> (Å)	6.872	6.967	6.897	9.465	9.023	7.545	21.293	21.581	21.930	
β	104.37	102.43	103.11	99.00	105.39	117.08				
rms % error		2.0	1.5		6.6	26.5		1.8	19.9	
lattice energy (kJ mol ⁻¹)	-96.7	-98.7	-97.4	-93.3	-99.5	-97.4	-102.96	-109.72	-97.2	

^a Minimizations with summation limits of 20 Å.

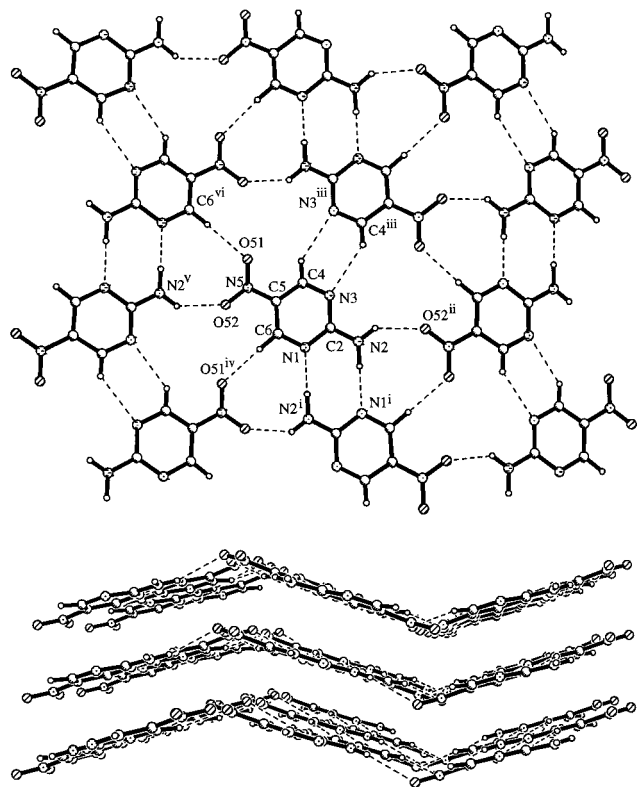


Figure 3. (a, top) Schematic view of the infinite 2-D hydrogen bonded layer for form **II**. Symmetry codes for nearest neighbors are (i) $-x, 1 - y, -z$; (ii) $1/2 - x, -1/2 + y, 1/2 - z$; (iii) $-1 - x, 1 - y, 1 - z$; (iv) $1/2 + x, 1/2 - y, -1/2 + z$; (v) $-1/2 - x, -1/2 + y, 1/2 - z$; (vi) $-1/2 + x, 1/2 - y, 1/2 + z$. (b, bottom) Edge-on view showing the buckling of the individual layers, dotted lines indicate hydrogen bonds.

are also interconnected via a pair of symmetry related C(4)–H(4)···O(51ⁱⁱ) hydrogen bonds.

Theoretical Crystal Structure Reproduction. The planar, layered assembly in form **I**, is satisfactorily reproduced using both the EXPTL and IDEAL molecular structures. The rms error in cell lengths is 1.5% when starting with the optimized molecular structure and 2.0% with the experimental molecular structure as a starting point, Table 3. The intermolecular potential has satisfactorily reproduced the unusually short distance between neighboring layers, including the overlap of $-NH_2$ groups and aromatic rings that takes place between molecules in adjacent layers. A recent study of interaction energies and crystal packing in form **I** and in 2-amino-5-nitropyridine has shown that close contacts in such compounds are mainly stabilized by dispersion forces, whereas the dominating forces within layers are primarily of electrostatic nature.¹⁶

In contrast, the buckled sheet in **II** (leading to a structure with a higher density than **I**) is poorly reproduced by the static minimization with this potential model, Table 3. Using the EXPTL molecular structure, the sheets unbuckle considerably

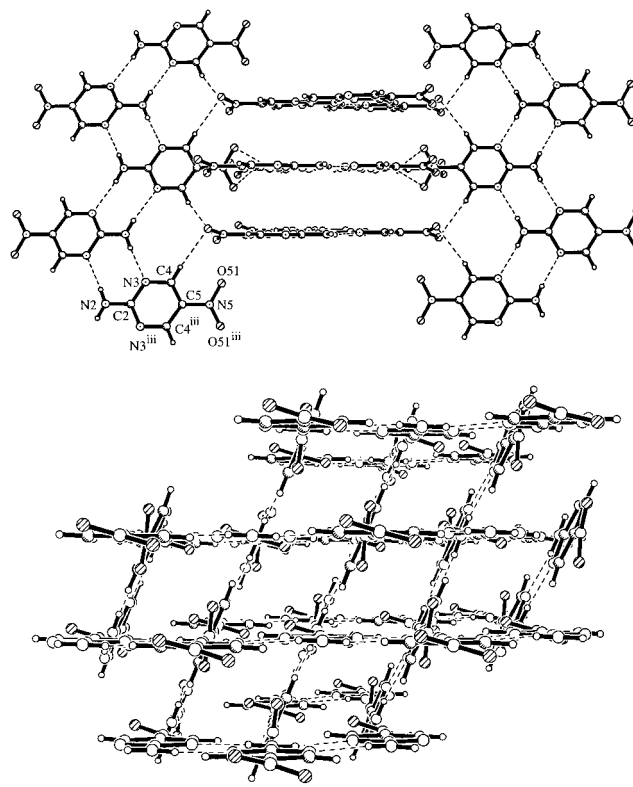


Figure 4. (a, top) Schematic view of the packing of the hydrogen bonded chains for form **III**; dotted lines indicate hydrogen bonds. Symmetry code (iii) $1/2 - x, 1/2 - y, z$. (b, bottom) Schematic view down the *c*-axis, showing the zigzag packing of ribbons in **III**.

to give a structure with only a slight buckle and stacked so that translationally related molecules overlap C–H and ring nitrogen atoms. The minimum energy structure has a density approaching that of forms **I** and **III**. When the IDEAL molecular structure is used, the sheets completely unbuckle and slide relative to each other, so that the minimization results in the planar sheet structure of **I**. The exact location of minima on a path of unbuckling the sheets and the relative translation of the sheets appears very sensitive to the details of the molecular structure. The unit cell expansion and unbuckling of the sheets indicate that the model potential is somewhat too repulsive in **II**, though only by a few kilojoules per mole, though there is no single atom–atom contact which stands out as being too repulsive. The course of the minimizations suggests that there is a low-energy pathway for the sliding of the near-planar sheets relative to each other.

The high-symmetry crystal structure in form **III** (space group *Pccn*) is well reproduced using the EXPTL molecular structure, with a r.m.s. error of 1.8% in the cell lengths, but not with the IDEAL molecular structure, Table 3. The bands of molecules held together by a zigzag network of parallel pairs of

Table 4. Ab Initio Calculations on Molecular Structures

source of structure	form I	form II	form III	ideal
<i>E</i> (SCF) /au	-521.215	-521.218	-521.211	-521.225
<i>E</i> (MP2)/au	-1.577	-1.574	-1.580	-1.564
<i>E</i> (total) /au	-522.792	-522.792	-522.791	-522.789
rel energy/kJ mol ⁻¹	0.58	0.00	2.24	9.08
bond lengths /Å ^a				
N(1)···C(2)	1.358	1.358	1.367	1.337
N(1)···C(6)	1.329	1.311	1.323	1.337
C(2)···N(2)	1.328	1.315	1.324	1.307
C(2)···N(3)	1.354	1.353	1.367	1.307
N(3)···C(4)	1.332	1.311	1.323	1.388
C(4)···C(5)	1.378	1.380	1.388	1.388
C(5)···N(5)	1.449	1.425	1.444	1.432
C(5)···C(6)	1.379	1.386	1.388	1.334
N(5)···O(51)	1.221	1.226	1.235	1.196
N(5)···O(52)	1.227	1.227	1.235	1.196

^a The bond lengths to the hydrogen atoms were standardized for all calculations.

N—H···N hydrogen bonds is reproduced well in both minimum energy structures. The bands stack parallel to each other, with the nitro groups at the edge of one band interacting closely with the nitro groups of the next band, stabilized by close C—H···O interactions which are only possible because the nitro group is twisted relative to the aromatic ring in the EXPTL molecular structure. The IDEAL molecular structure is unable to pack the coplanar nitro groups in the same way, thereby losing the stabilizing C—H···O contacts resulting in an expansion of the unit cell along the *c* axis. The minimum is found with the molecules of adjacent bands perpendicular to each other, with interactions between perpendicular nitro groups. The rotation of the bands to achieve this arrangement leads to large changes in the *a* and *b* parameters, and produces a significant expansion in the cell volume with a subsequent reduction in the lattice energy. Thus, the twist of the nitro group is essential to the stability of the crystal packing in this polymorph.

Energetics. The ab initio energies for the experimental molecular structures (EXPTL, with corrected hydrogen atom positions) and the SCF optimized ab initio structure are given in Table 4. The ab initio structure necessarily has the lowest energy at the SCF level at which it was optimized, but the experimental structures have a lower total energy. The differences are small, less than 0.03 Å in the bond lengths, but this is sufficient to affect the relative MP2 correlation energies. The difference in the relative energies of the experimental structures indicate that the molecule in form III, with the twisted nitro group, is about 2 kJ mol⁻¹ less stable than the planar molecular structures observed in I and II. This small difference for a rotation of 16° seems consistent with the experimental estimates of the barrier to rotation for the nitro group in nitrobenzene of only 17 ± 4 kJ mol⁻¹ from electron diffraction data,³⁰ 12.3 ± 1 kJ mol⁻¹ from microwave,³¹ and 13.6 kJ mol⁻¹ from Raman spectroscopy.³²

The lattice energies calculated for the experimental and minimized structures in Table 3 cover a small energy range. This result, in combination with the uncertainty in the model potential, and lack of a minimum closely corresponding to the buckled sheet structure make it difficult to estimate the relative stability of the polymorphs. Indeed, all three forms have the same lattice energy at the minimum obtained with the IDEAL molecular structure. The lattice energies for the EXPTL

minimized structures suggest that form III is the more stable than form I, even when the energy penalty required to twist the nitro group is taken into account. Form II is probably close in energy to form I, but all three structures are likely to fall in a range of less than 10 kJ mol⁻¹. This is consistent with the observation that all three forms have been obtained simultaneously from one solution.¹⁹

Prediction of Polymorphs. The lowest energy structures found by the search routine, Table 5, had a very similar cell volume/molecule and were only a few kilojoules per mole less stable than the minimum found starting from form I, using the same IDEAL molecular structure. The global minimum in the search (AV17) had the same sheet structure as I and II, being only slightly crinkled. The sheets stack to give a very similar coordination geometry to that found in the lattice energy minimum for EXPTL form II. Hence the packing appears to correspond to a low-energy point on the unbuckling and sheet translation pathway between the experimental structures of forms I and II. Thus, the search has essentially found the experimental packing forms I and II, within the errors of the potential energy surface and problems of minimization along such a surface.

Several other structures were found which were only marginally less stable. All but one of these contain molecules forming R₂²(8) dimers through pairs of symmetry related N(2)—H(21)···N(1) hydrogen bonds, with neighboring dimers linked by N(2)—H(22)···O(52) hydrogen bonds, as in the experimental structures of I and II. The one exception (CA13) still contained the same N(2)—H(21)···N(1) and N—H(22)···O(52) interactions, but they were very nonlinear and gave a P 1 structure with only single hydrogen-bond interactions between neighboring molecules. In some of the other P 1 structures, the dimers formed by pairs of N(2)—H(21)···N(1) hydrogen bonds were directly linked by N(2)—H(22)···O(52) hydrogen bonds to give planar ribbons. The edges of the ribbons have oxygen and hydrogen atoms protruding, and these packed with either close O···O contacts of 2.91 Å to form sheets (CA15), or with a vertical displacement between the ribbons (AB20). The dimeric N(2)—H(21)···N(1) motif deviated significantly from a planar arrangement in AK11, and the packing in AM5 was also quite complex and did not maintain the original P2₁/c symmetry.

Discussion

Given the abundance of hydrogen-bond donors and acceptors in 2-amino-5-nitropyrimidine, it is possible to envisage several different packing schemes, and successful predictions must obviously distinguish between alternative possible arrangements. Furthermore, we should also try to establish if some of the weaker contacts are merely the result of packing arrangements dictated by the stronger N—H···O and N—H···N hydrogen bonds, or if they actually can be considered as having a role in determining the overall structures. For example, in I and II, there is a single amine—nitro hydrogen bond (generated by the 2-fold screw axis) and a N—H···N dimeric interaction (across an inversion center); the appearance of the sheet is effectively determined by the distance between the center of inversion and the screw axis, the orientation of the molecule, and the length of *b*. It may then be concluded that the two short C—H···O and C—H···N contacts present in the layer are just accidental; i.e., they appear because there are no other ways in which a motif can form given the first two hydrogen bonds. However, if the amino—nitro interaction would involve O(51) instead of O(52), a far less satisfying layer would result, in particular, making it impossible to have any hydrogen bonds to C—H(6). Therefore, it would seem that the ostensibly weaker

(30) Domenicano, A.; Schultz, Gy.; Hargittai, I.; Colapietro, M.; Portalone, G.; George, P.; Bock, C. W. *Struct. Chem.* **1989**, *1*, 107.

(31) Hog, J. H. *A Study of Nitrobenzene*; Copenhagen, 1971.

(32) Carriera, L. A.; Towns, T. G. *J. Mol. Struct.* **1977**, *43*, 109.

Table 5. Comparison of Low-Energy Minima from Prediction Search with Those Obtained Starting from Experimental Structures^{a,b}

	energy/ kJ mol ⁻¹	N2–H21···N1/Å	N2–H22···O52/Å	cell volume/Z/Å ³	notes
forms I and II (IDEAL) ^c	–96.8	2.844	3.055	295.3	planar 2-D sheets
form III (IDEAL)	–96.9	2.913		311.6	perpendicular ribbons
AV17	–95.2	2.823	2.993	297.4	near-planar 2-D sheets
AB20	–94.0	2.841	2.950	295.2	ribbons
CA15	–94.5	2.865	2.980	292.5	ribbons positioned in layers
AK11	–94.6	2.841	2.958	299.1	molecules tilted about N2–H22···O22 bonds
AM5	–94.3	2.848	2.905	298.0	complex linkages by N2–H22···O22 bonds
CA13	–94.0	2.841	2.950	295.2	N2–H21···N1 bonds to different molecules

^a All minimizations with lattice energies summed to 15 Å. ^b Structure code denoted by MOLPAK reference to starting structure. ^c Values given for form **I**, but those of form **II** are virtually identical (cell volume difference of 0.01%).

interactions to C–H moieties have an active role to play in the assembly of the sheets in **I** and **II**.

Once the amino–nitro N–H···O hydrogen bond is abandoned, as in **III**, and the N–H···N motif is propagated into an infinite ribbon (made possible due to mirror symmetry), instead of having alternating N–H···N and C–H···N synthons as in **I** and **II**, it would seem less likely that a planar sheet can be constructed. Nitro groups are protruding from both sides of the ribbon, and it is not possible for those moieties to have access to any hydrogen-bond donors if the ribbons are put together in a coplanar fashion (this would result in very short –NO₂···O₂N– distances). In order for the remaining hydrogen-bond donor C–H(4) and acceptor O(51) to be satisfied, the ribbons have to be partially intercalated, resulting in an extended zigzag arrangement of neighboring ribbons, Figure 4b. The angle between ribbons (dictated by the glide plane), is ca. 65°. However, as noted above, one arrangement with coplanar ribbons (CA15) was predicted to be only slightly less stable than the observed structures which demonstrates the problems with trying to rationalize crystal packing only in terms of a few motifs; the resulting structure is a balance between all intermolecular interactions.

Since we have crystallized three centrosymmetric polymorphs of 2-amino-5-nitropyrimidine, the question arises whether there are hitherto undetected crystalline forms that appear in non-centrosymmetric structures. Both the existing structures and our calculations strongly suggest that such polymorphs are highly unlikely. First, the dimeric N–H···N hydrogen bonds, related by a center of inversion effectively rules out a polar structure. As this is the only motif present in all three forms, it seems reasonable to conclude that this synthon is the single most important intermolecular interaction. The N–H···N dimer is also present in 2-aminopyridine,³³ 2-aminopyrimidine,³⁴ and all three polymorphs of 2-amino-3-nitropyridine.³⁵ In addition, it has been demonstrated³⁶ that molecules related by inversion have fewer packing restrictions that motifs generated by glide planes or screw-axes even though the energetics of the latter motifs may be more favorable (as dimeric species). It is also possible to envisage an amino–nitro interaction involving two symmetry related N–H···O hydrogen bonds. However, such an interaction would effectively rule out the possibility of a N–H···N dimer. The dominance of the N–H···N dimer over a possible amino–nitro dimer can be rationalized in terms of geometry and linearity (in addition to the superior accepting

ability of the heterocyclic nitrogen atom); the N–H···N dimer with parallel N–H···N bonds optimizes the electrostatics of both interactions, whereas an amino–nitro dimer must yield a compromise imposed by the poor geometric complementarity of the amino and the nitro groups. The lack of an amino–nitro dimer in **I–III** as well as in 2,6-dichloro-4-nitroaniline,³⁷ 3-nitroaniline,³⁸ and 4-nitroaniline³⁹ (where there is no competition from an N–H···N dimer), would further indicate that such a motif is of lesser importance for crystal packing and assembly.

Second, our calculations yielded no low-energy structures without a center of symmetry which leads us to conclude that it is very unlikely that 2-amino-5-nitropyrimidine could crystallize in a noncentrosymmetric, SHG-active, structural arrangement.

All three forms of 2-amino-5-nitropyrimidine that we have identified (**I–III**) have shown themselves to be stable over several months at ambient temperature and pressure, and we have not observed any changes in crystal morphology or macroscopic appearance as a function of time. All three polymorphs can be obtained separately through a careful choice of solvent, or via sublimation. DSC measurements were performed on **I–III**, but these were inconclusive as to the nature of the thermodynamic interrelationship between these forms, as we were only able to detect broad endotherms in the 234–238 °C range without any distinctive indications of phase transitions prior to melting. We intend to carry out thermomicroscopy measurements⁴⁰ on this system to determine if these forms are enantiotropically or monotropically related.

Although this molecule itself is relatively simple with very limited flexibility (rotation of the amino or nitro groups with respect to the aromatic ring), our crystal structure modeling has shown that this structural system presents a considerable challenge to current models of structure prediction. The best such a prediction can do is to find the minima in the lattice energy (calculated using the assumed model potential) which are closest to the experimental structures, using a rigid molecular structure derived by theoretical calculations. The 2-amino-5-nitropyrimidine polymorphic system has shown up limitations of this crude static thermodynamic criterion as well as the assumed rigidity and intermolecular potential.

The SCF 6-31G** optimization used for the IDEAL structure is a relatively high-level model for the gas-phase structure of an organic molecule, and yet is not as accurate as the crystal structure determinations, as judged by the MP2 level energies. The difference may have contributed to the problems in

(33) Chao, M.; Schempp, E.; Rosenstein, R. D. *Acta Crystallogr., Sect. B* **1975**, *31*, 2922.

(34) Furberg, S.; Groggaard, J.; Smedsrud, B. *Acta Chem. Scand., Ser. B* **1979**, *33*, 715.

(35) Aakeröy, C. B.; Beatty, A. M.; Nieuwenhuyzen, M.; Zou, M. J. *Mater. Chem.* **1998**, *8*, 1385. Destro, R.; Pilati, T.; Simonetta, M. *Acta Crystallogr., Sect. B* **1975**, *31*, 2883.

(36) Brock, C. P.; Dunitz, J. D. *Chem. Mater.* **1994**, *6*, 1118.

(37) Hughes, D. L.; Trotter, J. *J. Chem. Soc. A* **1971**, 2181.

(38) Skapski, A. C.; Stevenson, J. L. *J. Chem. Soc., Perkin Trans. 2* **1973**, 1197.

(39) Colapietro, M.; Domenicano, A.; Marciantie, A.; Portalone, G. Z. *Naturforsch., Teil B* **1982**, *37*, 1309.

(40) Kuhnert-Brandstaetter, M. *Thermomicroscopy in the Analysis of Pharmaceuticals*; Pergamon Press: Oxford, 1971.

modeling the buckled sheet structure, form **II**. Any rigid molecule input structure would fail to predict the “twisted” infinite ribbons in form **III**. However, predicting crystal structures while allowing conformational flexibility not only increases the searching problem, but also depends on an accurate balance between the inter- and intramolecular potentials.⁴¹

The model intermolecular potential is also the current “state of the art”, and would have been judged very suitable for this system if only forms **I** and **III** had been identified and experimentally characterized. However, it fails to reproduce the dense buckled sheet structure of form **II**, suggesting that the potential is not producing the energy barrier to unbuckling. This is probably due to the potential being too repulsive, though its ability to reproduce the close intersheet contacts in form **I** and related molecules, plus the small energy change, suggests that the errors are small. The assumed isotropic atom–atom form for the repulsion may be inadequate for the stacked aromatic rings or hydrogen atom interactions as the distributed multipoles show that charge density in these regions is not spherical. Thus, the adequate modeling of form **II** may require the development of anisotropic atom–atom repulsion potentials for organic molecules.⁴² Nevertheless, the calculations indicate that there is a relatively low-energy pathway for transforming the planar form **I** to the buckled sheet form **II**, although there have been no experimental signs of phase transformations.

The failure of the intermolecular potential and rigid molecule model to produce a minimum in the lattice energy for one of the three polymorphs of 2-amino-5-nitropyrimidine clearly prevents the crystal structure prediction scheme from finding all known polymorphs. Since with this model potential and the gas-phase molecular model, the buckled form **II** transforms into the planar form **I**, lattice minimization searches could not predict **II** as separate from **I**. The minimum corresponding to the IDEAL structure for form **III** is low density and high symmetry, and thus unlikely to be found from the majority of search routines which consider only the common space groups with a complete molecule in the asymmetric unit, let alone those which use a close-packing criterion in searching for the starting points. However, this failure is not very significant since this minimum in the lattice energy is an artifact of the rigid molecule assumption and does not correspond to a plausible crystal structure.

It is clear that the conformational flexibility inherent in 2-amino-5-nitropyrimidine does play an important role in providing alternative packing arrangements and stability, and this is a good example of a system where a small change in molecular geometry can allow a qualitatively different and more

favorable crystal packing. The calculations confirm that a small energy change associated with a molecular distortion can be more than compensated for by increased density and stability of the crystal.

The crystal structure prediction scheme has been successful within the stated limitations, in that the basic sheet structure of forms **I** and **II** was found as the global minimum in the search. However, the prediction of other structures within a few kilojoules per mole in stability, when there has been no experimental signs of further polymorphs, shows that we cannot predict polymorphs solely on the basis of lattice energy minimization. It is quite common for crystal structure predictions schemes to find several plausible crystal structures of comparable lattice energy to the observed structure^{43,44} even when using this standard of accuracy in the model potential.^{6,45} Our calculations predict that ribbon structures are energetically feasible polymorphs, but they have not been found in the experimental search for possible polymorphs, which supports the conclusion that the computer prediction of polymorphism will require the consideration of other properties of the low-energy minima in the static lattice energy.⁶

This study has illustrated the complexities involved with predicting the structures of even relatively simple organic molecules. State-of-the-art models have been reasonably successful in finding low-energy structures that correspond to experimentally observed polymorphs. Nevertheless, to improve our understanding of this complex phenomenon, more refined potential models need to be developed, and more structural and accurate thermodynamic data are required.

Acknowledgment. To Dr. Sam Motherwell for useful discussions and Mr. Giovanni di Gregorio for some preliminary studies (as an undergraduate project student). We acknowledge financial support from NSF-EPSCoR (OSR-9550487), DuPont, NIDevR, and the EPSRC.

Supporting Information Available: Crystallographic details for **I–III**, including descriptions of structure determinations, tables of atomic coordinates and isotropic thermal parameters, bond lengths and angles, anisotropic thermal parameters and details about parameters for the 6-exp potential used (11 pages, print/PDF). See any current masthead page for ordering information and Web access instructions.

JA981122I

(43) Gavezzotti, A.; Filippini, G.; Kroon, J.; van Eijck, B. P.; Klewinghaus, P. *Chem.—Eur. J.* **1997**, *3*, 893.

(44) Payne, R. S.; Roberts, R. L.; Rowe, R. C.; Docherty, R. *J. Comput. Chem.* **1998**, *19*, 1.

(45) Mooij, W. T. M.; van Eijck, B. P.; Price, S. L.; Verwer, P.; Kroon, J. *J. Comput. Chem.* **1998**, *19*, 459.

(41) Gavezzotti, A. In *Theoretical Aspects and Computer Modeling of the Molecular Solid State. The Molecular Solid State*; Gavezzotti, A., Ed.; John Wiley: Chichester, 1997.

(42) Price, S. L. *Phil. Mag. B* **1996**, *73*, 95.